


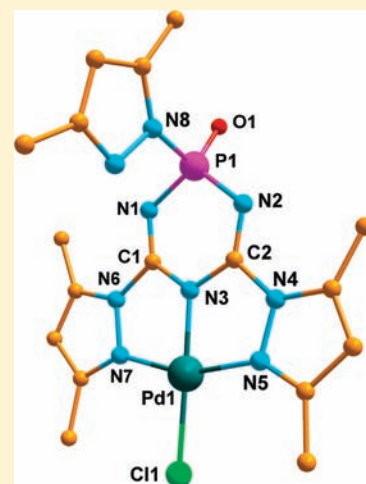
Carbophosphazene-Supported Ligand Systems Containing Pyrazole/Guanidine Coordinating Groups[#]

Vadapalli Chandrasekhar,* Venkatasubbiah Krishnan, Ramachandran Azhakar, Tapas Senapati, Atanu Dey, and R. Suriya Narayanan

Department of Chemistry, Indian Institute of Technology Kanpur, Kanpur-208016, India

 Supporting Information

ABSTRACT: Carbophosphazene-based coordination ligands [$\{\text{NC}(\text{NMe}_2)_2\}_2\{\text{NP}(3,5\text{-Me}_2\text{Pz})_2\}$] (1), [$\{\text{NC}(\text{NEt})_2\}\{\text{NC}(3,5\text{-Me}_2\text{Pz})\}\{\text{NP}(3,5\text{-Me}_2\text{Pz})_2\}$] (2), [$\{\text{NC}(3,5\text{-Me}_2\text{Pz})_2\}_2\{\text{NP}(3,5\text{-Me}_2\text{Pz})_2\}$] (3), [$\{\text{NC}(\text{OC}_5\text{H}_4\text{N})\}_2\{\text{NP}(\text{NC}(\text{NMe}_2)_2)_2\}$] (4), and [$\{\text{NC}(\text{OC}_5\text{H}_4\text{N})\}_2\{\text{NP}(\text{NC}(\text{NMe}_2)_2)_2\}$] (5) were synthesized and structurally characterized. In these compounds, the six-membered $\text{C}_2\text{N}_3\text{P}$ ring is perfectly planar. The reaction of 1 with CuCl_2 afforded [$\{\text{NC}(\text{NMe}_2)_2\}_2\{\text{NHP}(\text{O})(3,5\text{-Me}_2\text{Pz})\}\cdot\{\text{Cu}(3,5\text{-Me}_2\text{PzH})_2(\text{Cl})\}$] [Cl] (6). The ligand binds to Cu(II) utilizing the geminal [$\text{P}(\text{O})(3,5\text{-Me}_2\text{Pz})$] coordinating unit. Similarly, the reaction of 2 with PdCl_2 afforded, after a metal-assisted P–N hydrolysis, [$\{\text{NC}(\text{NEt})_2\}\{\text{NC}(3,5\text{-Me}_2\text{Pz})\}\{\text{NP}(\text{O})(3,5\text{-Me}_2\text{Pz})\}\cdot\{\text{Pd}(3,5\text{-Me}_2\text{PzH})(\text{Cl})\}$] (7). In the latter, the [$\text{P}(\text{O})(3,5\text{-Me}_2\text{Pz})$] unit does not coordinate; in this instance, the Pd(II) is bound by a ring nitrogen atom and a carbon-tethered pyrazolyl nitrogen atom. The reaction of 3 with PdCl_2 also results in P–N bond hydrolysis affording [$\{\text{NC}(3,5\text{-Me}_2\text{Pz})_2\}\{\text{NP}(\text{O})(3,5\text{-Me}_2\text{Pz})\}\{\text{Pd}(\text{Cl})\}$] (8). In contrast to 7, however, in 8, the Pd(II) elicits a nongeminal η^3 coordination from the ligand involving two carbon-tethered pyrazolyl groups and a ring nitrogen atom. Metalated products could not be isolated in the reaction of 3 with K_2PtCl_4 . Instead, a P–O–P bridged carbodiphosphazene dimer, [$\{\text{NC}(3,5\text{-Me}_2\text{Pz})\text{NHC}(3,5\text{-Me}_2\text{Pz})\}\{\text{NP}(\text{O})\}_2$] (9), was isolated as the major product. Finally, the reaction of 5 with PdCl_2 resulted in [$\{\text{NC}(\text{OC}_5\text{H}_4\text{N})\}_2\{\text{NP}(\text{NC}(\text{NMe}_2)_2)_2\}\cdot\{\text{PdCl}_2\}$] (10). In the latter, the exocyclic P–N bonds are quite robust and are involved in binding to the metal ion. Compounds 6–10 have been characterized by a variety of techniques including X-ray crystallography. In all of the compounds, the bond parameters of the inorganic heterocyclic rings are affected by metalation.

**INTRODUCTION**

Cyclophosphazenes are an important family of inorganic ring systems which have received attention for a variety of reasons.¹ These include mechanistic studies involving the nucleophilic substitution reactions of halogenocyclophosphazenes,² the polymer chemistry based on a $\text{P}=\text{N}$ backbone¹ or on an organic backbone containing cyclophosphazene pendant groups,³ and studies on the coordination chemistry of cyclophosphazene ligands.⁴ This last aspect has engaged our attention for some years, and we and others have successfully demonstrated the utility of the cyclophosphazene ring to support multitopic coordination platforms.⁴ In view of this success, we turned our attention to cyclocarbophosphazenes, which can be considered as hybrid systems of the organic heterocyclic rings, *s*-triazines, and the inorganic heterocyclic rings, cyclophosphazenes.⁵ In a preliminary study, carried out a few years ago, we showed that a pyrazolyl carbophosphazene, upon interaction with Cu(II) ions, undergoes selective P–N bond cleavage, without affecting the C–N bonds, and affords novel tetranuclear copper(II) assemblies.⁶ We have since elaborated upon this work and report these findings in this paper. Our observations suggest that

pyrazolyl carbophosphazenes are indeed prone to metal-assisted P–N bond hydrolysis under a variety of metalation conditions. In one case, we have also been able to isolate a dicarbophosphazene containing a P–O–P bond. Concomitant with these studies we have endeavored to search for robust carbophosphazene ligands where the P–N bond would remain *intact* even *after* metalation. Another aspect of interest was to be able to find reagents that would preferentially react at the phosphorus site and leave the carbon site untouched. We have found that reactions of 1,1,3,3-tetramethylguanidine with the chlorocarbophosphazene, [$\{\text{NCCl}\}_2\{\text{NP}(\text{Cl})_2\}$], occur regioselectively at the phosphorus site. Further, our investigations revealed that the carbophosphazene ligand containing guanidine substituents, [$\{\text{NC}(p\text{-OC}_5\text{H}_4\text{N})\}_2\{\text{NP}(\text{NC}(\text{NMe}_2)_2)_2\}$], is quite robust, and the ligand framework remains intact even after metalation. Accordingly, this manuscript describes the synthesis and structural characterization of [$\{\text{NC}(\text{NMe}_2)_2\}_2\{\text{NP}(3,5\text{-Me}_2\text{Pz})_2\}$] (1), [$\{\text{NC}(\text{NEt})_2\}\{\text{NC}(3,5\text{-Me}_2\text{Pz})\}\{\text{NP}(3,5\text{-Me}_2\text{Pz})_2\}$] (2),

Received: December 3, 2010

Published: February 16, 2011

Table 1. Crystal and Refinement Data for 1–5

parameter	1	2	3	4	5
formula	C ₁₆ H ₂₆ N ₉ P	C ₂₁ H ₃₁ N ₁₀ P	C ₂₂ H ₂₈ N ₁₁ P	C ₁₂ H ₂₄ Cl ₂ N ₉ P	C ₃₀ H ₇₆ N ₂₂ O ₇ P ₂
fw	375.43	454.53	477.52	396.27	1159.27
temp (K)	293(2) K	100(2) K	213(2) K	100(2) K	153(2) K
wavelength	0.71073 Å	0.71073 Å	0.71073 Å	0.71069 Å	0.71069
cryst syst	monoclinic	monoclinic	monoclinic	monoclinic	monoclinic
space group	Cc	C2/c	C2/c	P2 ₁ /n	C2/c
unit cell dimensions	<i>a</i> = 15.762(4) Å <i>b</i> = 8.8893(16) Å <i>c</i> = 14.129(3) Å α = 90° β = 90.822(16)° γ = 90°	<i>a</i> = 26.786(17) Å <i>b</i> = 10.754(7) Å <i>c</i> = 16.522(10) Å α = 90° β = 101.437(10)° γ = 90°	<i>a</i> = 29.729(5) Å <i>b</i> = 10.744(2) Å <i>c</i> = 15.486(3) Å α = 90° β = 100.29(2)° γ = 90°	<i>a</i> = 10.549(5) Å <i>b</i> = 13.494(5) Å <i>c</i> = 13.764(5) Å α = 90° β = 105.902(5)° γ = 90°	<i>a</i> = 24.580(5) Å <i>b</i> = 11.104(5) Å <i>c</i> = 22.363(5) Å α = 90° β = 107.644(5)° γ = 90°
V/Å ³ , Z	1979.5(7), 4	4664.6(5), 8	4866.8(15), 8	1884.3(13), 4	5817(3), 4
<i>d</i> _c /Mg m ⁻³	1.260	1.294	1.303	1.397	1.324
abs. coeff.	0.159 Mm ⁻¹	0.149 Mm ⁻¹	0.147 Mm ⁻¹	0.445 Mm ⁻¹	0.144 Mm ⁻¹
F (000)	800	1936	2016	832	2464
cryst size (mm)	0.45 × 0.56 × 0.62	0.7 × 0.7 × 0.6	0.4 × 0.3 × 0.3	0.10 × 0.08 × 0.06	0.12 × 0.09 × 0.08
θ range/deg	2.58 to 27.50°	1.55 to 28.31°	2.79 to 24.21	2.16 to 28.31°	2.16 to 26.00°
limiting indices	0 ≤ <i>h</i> ≤ 20, 0 ≤ <i>k</i> ≤ 11, −18 ≤ <i>l</i> ≤ 18	−21 ≤ <i>h</i> ≤ 35, −14 ≤ <i>k</i> ≤ 14, −21 ≤ <i>l</i> ≤ 21	−32 ≤ <i>h</i> ≤ 31, −12 ≤ <i>k</i> ≤ 12, −17 ≤ <i>l</i> ≤ 17	−14 ≤ <i>h</i> ≤ 8, −18 ≤ <i>k</i> ≤ 17, −18 ≤ <i>l</i> ≤ 18	−30 ≤ <i>h</i> ≤ 30, −13 ≤ <i>k</i> ≤ 13, −27 ≤ <i>l</i> ≤ 19
reflns collected	2363	13951	15112	12163	15889
reflns unique [Rint]	2361 [0.0621]	5341 [0.0168]	3719 [0.0309]	4639 [0.0430]	5700 [0.0461]
completeness to θ	100.0% (27.50°)	91.9% (28.31°)	94.9% (24.21°)	99.0% (28.31°)	99.7% (26.00°)
data/restraints/params	2361/2/270	5341/0/298	3719/0/315	4639/0/225	5700/0/376
GoF on F ²	1.071	1.026	1.053	1.108	1.068
final R indices [I > 2σ(I)]	R1 = 0.0334, wR2 = 0.0836	R1 = 0.0459, wR2 = 0.1257	R1 = 0.0316, wR2 = 0.0833	R1 = 0.0514, wR2 = 0.1345	R1 = 0.0560, wR2 = 0.1421
R indices (all data)	R1 = 0.0366, wR2 = 0.0857	R1 = 0.0507, wR2 = 0.1305	R1 = 0.0411, wR2 = 0.0881	R1 = 0.0842, wR2 = 0.2037	R1 = 0.0735, wR2 = 0.1621
largest residual peaks	0.233 and −0.169 e Å ⁻³	0.610 and −0.388 e Å ⁻³	0.176 and −0.274 e Å ⁻³	0.552 and −0.693 e Å ⁻³	0.750 and −0.317 e Å ⁻³

[NC(3,5-Me₂Pz)]₂[NP(3,5-Me₂Pz)₂] (3), [{NCCl}₂NP(NC(NMe₂)₂)₂] (4), [{NC(*p*-OC₅H₄N)}₂NP(NC(NMe₂)₂)₂] (5), [{NC(NMe₂)₂}{NHP(O)(3,5-Me₂Pz)} · {Cu(3,5-Me₂PzH)₂(Cl)}][Cl] (6), [{NC(NEt)₂}{NC(3,5-Me₂Pz)}{NP(O)(3,5-Me₂Pz)} · {Pd(3,5-Me₂PzH)(Cl)}] (7), [{NC(3,5-Me₂Pz)₂}-{NP(O)(3,5-Me₂Pz)}{Pd(Cl)}] (8), [{NC(3,5-Me₂Pz)NHC(3,5-Me₂Pz)}{NP(O)}₂] (9), and [{NC(OC₅H₄N)}₂NP(NC(NMe₂)₂)₂ · {PdCl₂}] (10).

EXPERIMENTAL SECTION

General. Solvents and other general reagents used in this work were purified according to standard procedures.⁷ [{NCCl}₂{NP(NC(NMe₂)₂)₂}]₂ (1), *N,N,N',N'*-tetramethylmethylenediamine,⁹ [{NC(NMe₂)₂}{NP(NC(NMe₂)₂)₂}]₂ (2), and 3,5-dimethylpyrazole⁷ were prepared according to literature procedures. CuCl₂ (Lancaster), PdCl₂(PhCN)₂ (Aldrich, U.S.A.), NaN(CN)₂ (Aldrich, U.S.A.), 1,1,3,3-tetramethylguanidine (Aldrich, U.S.A.), PCl₅ (Aldrich, U.S.A.), dimethylamine (SD Fine, India), and formaldehyde (SD Fine, India) were used as obtained.

Instrumentation. ¹H and ³¹P NMR spectra were recorded in CDCl₃ solutions on a JEOL spectrometer operating at 400.0 and 161.7 MHz, respectively. Chemical shifts are reported with respect to internal tetramethylsilane (¹H) and external 85% H₃PO₄ (³¹P). Mass spectra were recorded on a JEOL SX 102/DA 6000 mass spectrometer using

xenon (6 kV, 10 mA) as the FAB gas. IR spectra were recorded as KBr pellets on a Bruker Vector 22 FT IR spectrophotometer operating from 400 to 4000 cm⁻¹. EPR spectra were recorded on a Varian 109E Line Century Series X-band spectrometer, at liquid nitrogen temperature. Electronic spectra were recorded on a Perkin-Elmer-Lambda 20 UV-vis spectrometer and on a Shimadzu UV-160 spectrometer using CH₂Cl₂ as the solvent. Elemental analyses of the compounds were obtained using a Thermoquest CE instruments CHNS-O, EA/110 model.

X-Ray Crystallography. The crystal data and the cell parameters for compounds 1–10 are given in Tables 1 and 2. Single crystals suitable for X-ray crystallographic analyses were obtained by slow evaporation of various organic solvents (see Experimental Section). The crystal data for compounds 1–10 have been collected on a Bruker SMART CCD diffractometer using a Mo Kα sealed tube. The program SMART^{11a} was used for collecting frames of data, indexing reflections, and determining lattice parameters; SAINT^{11a} for integration of the intensity of reflections and scaling; SADABS^{11b} for absorption correction; and SHELXTL^{11c,d} for space group and structure determination and least-squares refinements on F². All of the structures were solved by direct methods using the program SHELXS-97^{11e} and refined by full-matrix least-squares methods against F² with SHELXL-97.^{11e} Hydrogen atoms were fixed at calculated positions, and their positions were refined with a riding model. All non-hydrogen atoms were refined with anisotropic displacement parameters. The crystallographic figures have been generated using the *Diamond 3.2f* software.^{11f}

Table 2. Crystal and Refinement Data for 6–10

parameter	6	7	8	9	10
formula	C ₂₂ H ₃₈ Cl ₄ CuN ₁₁ OP	C ₂₈ H ₃₇ ClN ₁₁ OP Pd	C ₁₈ H ₂₃ Cl ₃ N ₉ OP Pd	C ₃₁ H ₃₀ N ₁₄ O ₃ P ₂	C ₂₂ H ₃₂ Cl ₂ N ₁₁ O ₂ P Pd
fw	708.94	716.51	625.17	708.63	690.86
temp (K)	100(2) K	213(2) K	100(2) K	298(2) K	100(2) K
wavelength	0.71073 Å	0.71073 Å	0.71069 Å	0.71073 Å	
cryst syst	triclinic	monoclinic	triclinic	monoclinic	triclinic
space group	$P\bar{1}$	$I2/a$	$P\bar{1}$	$P2/n$	$P\bar{1}$
unit cell dimensions	$a = 11.5158(7)$ Å $b = 11.8370(7)$ Å $c = 12.1809(7)$ Å $\alpha = 85.4340(10)^\circ$ $\beta = 81.8010(10)^\circ$ $\gamma = 78.7550(10)^\circ$	$a = 15.657(2)$ Å $b = 25.340(3)$ Å $c = 16.686(3)$ Å $\alpha = 90^\circ$ $\beta = 95.464(18)^\circ$ $\gamma = 90^\circ$	$a = 9.428(5)$ Å $b = 10.069(5)$ Å $c = 13.778(5)$ Å $\alpha = 91.341(5)^\circ$ $\beta = 106.311(5)^\circ$ $\gamma = 109.631(5)^\circ$	$a = 11.914(4)$ Å $b = 11.094(3)$ Å $c = 12.800(4)$ Å $\alpha = 90^\circ$ $\beta = 110.904(5)^\circ$ $\gamma = 90^\circ$	$a = 9.600(8)$ Å $b = 11.027(9)$ Å $c = 15.181(12)$ Å $\alpha = 90.1880(10)^\circ$ $\beta = 98.775(10)^\circ$ $\gamma = 113.980(10)^\circ$
$V/\text{Å}^3, Z$	1609.59(16), 2	6590.0(17), 8	1172.3(10), 2	1580.4(8), 2	1447.4(2), 2
$d_c/\text{Mg m}^{-3}$	1.463	1.444	1.771	1.489	1.585
abs. coeff.	1.097 Mm^{-1}	0.733 Mm^{-1}	1.234 Mm^{-1}	0.198 Mm^{-1}	0.923 Mm^{-1}
F (000)	734	2944	628	736	704
cryst size (mm)	0.35 × 0.15 × 0.10	0.30 × 0.30 × 0.25	0.2 × 0.15 × 0.1	0.2 × 0.15 × 0.15	0.09 × 0.07 × 0.05
θ range/deg	1.69 to 28.29°	1.47 to 22.46°	1.55 to 28.31	2.50 to 28.48	2.36 to 26.00°
limiting indices	$-15 \leq h \leq 15,$ $-15 \leq k \leq 7,$ $-15 \leq l \leq 15$	$-16 \leq h \leq 16,$ $-27 \leq k \leq 27,$ $-17 \leq l \leq 17$	$-12 \leq h \leq 12,$ $-11 \leq k \leq 13,$ $-11 \leq l \leq 18$	$-15 \leq h \leq 7,$ $-13 \leq k \leq 14,$ $-17 \leq l \leq 16$	$-7 \leq h \leq 11,$ $-13 \leq k \leq 13,$ $-18 \leq l \leq 18$
reflns collected	10126	16803	7589	10238	8120
reflns unique [Rint]	7062 [0.0500]	4222 [0.1448]	5288 [0.0318]	3913 [0.0250]	5559 [0.0261]
completeness to θ	88.4% (28.29°)	98.4% (22.46°)	90.5% (28.31)	97.6% (28.48)	97.7% (26.00°)
data/restraints/params	7062/0/383	4222/66/385	5288/0/304	3913/0/217	5559/0/360
GoF on F^2	0.970	0.866	0.986	1.101	1.129
final R indices [$I > 2\sigma(I)$]	R1 = 0.0380, wR2 = 0.0936	R1 = 0.0640, wR2 = 0.1385	R1 = 0.0467, wR2 = 0.0982	R1 = 0.0667, wR2 = 0.1881	R1 = 0.0426, wR2 = 0.1077
R indices (all data)	R1 = 0.0474, wR2 = 0.0966	R1 = 0.1102, wR2 = 0.1528	R1 = 0.0626, wR2 = 0.1048	R1 = 0.0777, wR2 = 0.1988	R1 = 0.0526, wR2 = 0.1313
largest residual peaks	0.897 and -0.473 e.Å^{-3}	1.397 and -0.708 e.Å^{-3}	0.905 and 0.733 e.Å^{-3}	0.615 and -0.607 e.Å^{-3}	1.205 and -0.673 e.Å^{-3}

Synthesis. $[\{NC(NMe_2)\}_2\{NP(3,5-Me_2Pz)_2\}]$ (**1**). A solution of the sodium salt of 3,5-dimethylpyrazole prepared by the reaction of NaH (0.36 g, 15.2 mmol) and 3,5-dimethylpyrazole (1.46 g, 15.2 mmol) was taken in tetrahydrofuran (50 mL) and added dropwise to a solution of $[\{NC(NMe_2)\}_2\{NP(3,5-Me_2Pz)_2\}]$ (1.95 g, 7.6 mmol) in tetrahydrofuran (50 mL) at room temperature. The reaction mixture was subsequently heated under reflux for 24 h, allowed to cool, and filtered through a G4 frit containing Celite. Removal of the solvent from the filtrate in vacuo afforded a pale yellow precipitate. This was subjected to column chromatography on a neutral alumina column using dichloromethane as the eluent to obtain pure **1**. Yield: 1.82 g (64%). Mp. 162–164 °C. ^1H NMR: δ 2.23, 2.11 (s, 12H, Pz-CH₃), 3.05 (s, 12H, -NMe₂), 5.83 (s, 2H, Pz-CH). $^{31}\text{P}\{^1\text{H}\}$ NMR: δ 24.0 (s). MS(FAB): 376(M^+). IR (KBr) cm^{-1} : 3109 (w), 2926 (m), 2863 (m), 1474 (s), 1375 (s), 1300 (s), 1263 (m), 1169 (s), 1147 (s), 1060 (s), 983 (s), 927 (s), 808 (m), 766 (s), 612 (m), 570 (s), 552 (s). Anal. Calcd. for C₁₆H₂₆N₉P: C, 51.18; H, 6.98; N, 33.57. Found: C, 51.25; H, 6.12; N, 31.92.

$[\{NC(NMe_2)\}_2\{NC(3,5-Me_2Pz)\}\{NP(3,5-Me_2Pz)_2\}]$ (**2**). To a solution of $[\{NC(NMe_2)\}_2\{NP(3,5-Me_2Pz)_2\}]$ (1.5 g, 6.3 mmol) in toluene in an ice-bath was added dropwise a solution of 3,5-dimethylpyrazole (2.41 g, 25.1 mmol) and triethylamine (2.56 g, 25.1 mmol) over a period of 15 min. The mixture was refluxed for 24 h, cooled, and filtered through a G4 frit. Removal of solvent from the filtrate in vacuo afforded a precipitate. This was subjected to column chromatography on a neutral alumina column

using ethyl acetate/*n*-hexane (95:5) as the eluant to obtain pure **2**. Yield: 1.20 g (42%). Mp. 119–121 °C. ^1H NMR: δ 1.22 (t, 6H, N-CH₂-CH₃), 2.19, 2.25, 2.31 (s, 18H, Pz-CH₃), 3.65 (q, 4H, -N-CH₂-CH₃), 5.83 (s, 2H, Pz-CH). $^{31}\text{P}\{^1\text{H}\}$ NMR: δ 22.7 (s). MS(FAB): 455(M^+). IR (KBr) cm^{-1} : 3089 (w), 2979 (m), 2927 (m), 2870 (w), 1654 (m), 1513 (m), 1464 (m), 1389 (s), 1294 (s), 1225 (m), 1173 (s), 1149 (s), 1091 (s), 1009 (m), 965 (s), 923 (m), 829 (m), 772 (m), 634 (m), 580 (s). Anal. Calcd. for C₂₁H₃₁N₁₀P: C, 55.49; H, 6.87; N, 30.82. Found: C, 54.25; H, 6.24; N, 31.02.

$[NC(3,5-Me_2Pz)]_2[NP(3,5-Me_2Pz)_2]$ (**3**). To a solution of $[\{NC(3,5-Me_2Pz)\}_2\{NP(3,5-Me_2Pz)_2\}]$ (4.34 g, 18.0 mmol) in toluene (30 mL) in an ice-bath was added dropwise a solution of 3,5-dimethylpyrazole (6.91 g, 72.6 mmol) and pyridine (6.05 g, 72.0 mmol) in toluene (60 mL) over a period of 15 min. The mixture was refluxed for 24 h, cooled, and filtered through a G4 frit. Removal of the solvent from the filtrate in vacuo afforded a precipitate. This was subjected to column chromatography on a neutral alumina column using ethyl acetate/*n*-hexane (95:5) as the eluant to obtain pure **3**. Yield: 3.51 g (41%). Mp. 180–182 °C. ^1H NMR (CDCl₃, δ): 2.14, 2.22, 2.67 (s, 24H, Pz-CH₃), 5.93 (s, 4H, Pz-CH). $^{31}\text{P}\{^1\text{H}\}$ NMR (CDCl₃, δ): δ 22.4 (s). FAB-MS (m/e): 478 ($M + 1$)⁺. IR (KBr, cm^{-1}): 3081 (w), 2982 (m), 2926 (m), 2350 (w), 1585 (s), 1529 (s), 1475 (s), 552 (s). Anal. Calcd. for C₁₆H₂₆N₉P (%): C, 51.18; H, 6.98; N, 33.57. Found: C, 51.25; H, 6.12; N, 31.92.

$[\{NC\Cl\}_2\{NP(NC(NMe_2)_2)_2\}]$ (**4**). To a solution of $[\{NC\Cl\}_2\{NP\Cl_2\}]$ (7.2 g, 30 mmol) in tetrahydrofuran (70 mL) was added dropwise a solution of 1,1,3,3-tetramethyl-guanidine (15.1 g, 131 mmol) over a period of 30 min at 0–5 °C. The reaction mixture was subsequently stirred at room temperature for 24 h and filtered through a G4 frit. Removal of the solvent from the filtrate in vacuo afforded a colorless precipitate. This was dissolved in a small amount of acetonitrile and kept at 4 °C. After 12 h, a colorless crystalline product (**3**) was obtained. Yield: 9.1 g (75.5%). Mp. 140 °C. 1H NMR: δ 2.86 (s, 24H, NMe₂). $^{31}P\{^1H\}$ NMR: δ -3.9 (s). ESI-MS m/z , ion: 396.13. IR (KBr) cm^{-1} : 3406 (b), 3008 (s), 2934 (m), 2160 (w), 1632 (s), 1525 (s), 1470 (m), 1403 (s), 1385 (s), 1341 (m), 1261 (s), 1154 (s), 1060 (m), 983 (s), 948 (s), 919 734 (m), 722 (s), 647 (m), 531 (m), 467 (m). Anal. Calcd. for C₁₂H₂₄Cl₂N₉P (395.13): C, 36.37; H, 6.10; N, 31.81. Found: C, 36.42; H, 6.18; N, 31.72.

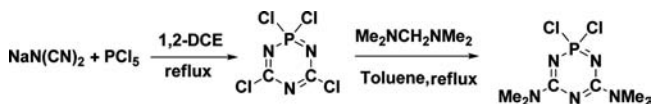
$[\{NC(p-OC_5H_4N)\}_2\{NP(NC(NMe_2)_2)_2\}]$ (**5**). An acetone solution (50 mL) of 4-hydroxy pyridine (2.0 g, 21 mmol) and an excess of K₂CO₃ (8.7 g, 63 mmol) was stirred for 1 h at room temperature in a N₂ atmosphere. To this solution was added $[\{NC\Cl\}_2\{NP\Cl_2\}]$ (4.0 g, 10.0 mmol), and the solution was heated under reflux for 48 h. Removal of the solvent at low pressure afforded a colorless residue. This was redissolved in dichloromethane (100 mL) and filtered using a G-4 frit. The light brown-colored solution, thus obtained, was concentrated to 10 mL and kept at 4 °C overnight. A colorless crystalline needle-shaped product resulted. Yield: 4.3 g (83%). Mp. 75 °C. 1H NMR: δ 2.86 (s, 24H, NMe₂), 6.32 (d, 4H, aromatic), 8.74 (d, 4H, aromatic). $^{31}P\{^1H\}$ NMR: δ 1.5 (s). ESI-MS m/z , ion: 514.25. IR (KBr) cm^{-1} : 3395 (b), 3107 (w), 2928 (m), 1636 (s), 1563 (s), 1389 (m), 1342 (s), 1298 (s), 1180 (m), 1126 (s), 975 (m), 854 (m), 767 (m), 723 (m), 668 (m), 611 (m), 581 (m), 556 (m), 469 (m). Anal. Calcd. for C₂₂H₃₂N₁₁O₂P (513.25): C, 51.45; H, 6.28; N, 30.00. Found: C, 51.57; H, 6.32; N, 29.91.

$[\{NC(NMe_2)_2\}_2\{NHP(O)(3,5-Me_2Pz)\} \cdot \{Cu(3,5-Me_2PzH)_2(Cl)\}][Cl]$ (**6**). To a solution of ligand **1** (0.056 g, 0.15 mmol) in dichloromethane (40 mL) was added anhydrous CuCl₂ (0.02 g, 0.15 mmol). After stirring for 12 h at room temperature, the reaction mixture was filtered and concentrated to a volume of 3 mL. To this solution was added 10 mL of *n*-hexane, upon which a solid was deposited. This was filtered and dried. Yield: 0.053 g (57%). Mp. 106–108 °C. UV/Visible: (CH₂Cl₂; λ_{max}/nm ($\epsilon_{max}/M^{-1}cm^{-1}$): 823(125), 467(625), 331(shoulder; 2107), 241(30 000). Solution magnetic moment, $\mu_B = 1.51 \mu_B$ (after applying diamagnetic corrections). EPR (CH₂Cl₂/toluene, 1:1, 77K): $g_{\parallel} = 2.27$; $g_{\perp} = 2.08$; $A_{\parallel} = 130 \times 10^{-4} cm^{-1}$. IR (KBr) cm^{-1} : 2927 (m), 1607 (s), 1559 (s), 1405 (m), 1330 (m), 1293 (m), 1219 (m), 1177 (s), 1050 (s), 987 (m), 954 (m), 929 (m), 902 (m), 822 (m), 598 (s), 556 (s). Anal. Calcd. for C₂₁H₃₆N₁₁POCuCl₂ (622.15): C, 40.42; H, 5.81; N, 24.69. Found: C, 39.56; H, 5.92; N, 25.72.

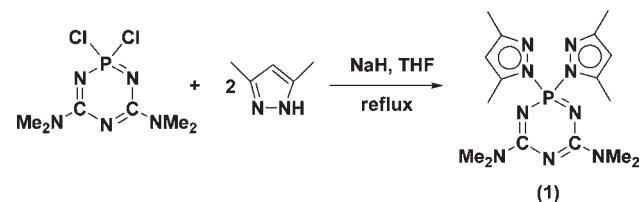
$[\{NC(NEt_2)_2\}_2\{NC(3,5-Me_2Pz)\}_2\{NP(O)(3,5-Me_2Pz)\} \cdot \{Pd(3,5-Me_2PzH)(Cl)\}]$ (**7**). To a solution of ligand **2** (0.10 g, 0.22 mmol) in dichloromethane (40 mL) was added Pd(PhCN)₂Cl₂ (0.08 g, 0.22 mmol). After stirring for 12 h at room temperature, the reaction mixture was filtered and concentrated to a volume of 3 mL. To this solution was added 10 mL of *n*-hexane, upon which a solid was deposited. This was filtered and dried. Yield: 0.11 g (84%). Mp. 70–72 °C. IR (KBr) cm^{-1} : 2977 (m), 2929 (m), 2856 (w), 1653 (m), 1586 (s), 1478 (m), 1419 (m), 1300 (s), 1237 (m), 1083 (s), 967 (s), 896 (s), 806 (m), 749 (m), 607 (m), 552 (m). UV/Visible: (CH₂Cl₂; λ_{max}/nm ($\epsilon_{max}/M^{-1}cm^{-1}$): 793(15), 386(shoulder; 269), 257(14,676). Anal. Calcd. for C₂₁H₃₂N₁₀POPdCl (612.12): C, 41.11; H, 5.25; N, 22.83. Found: C, 40.90; H, 4.98; N, 22.01.

$[\{NC(3,5-Me_2Pz)_2\}_2\{NP(O)(3,5-Me_2Pz)\}_2\{Pd(Cl)\}]$ (**8**). To a solution of $[\{NC(3,5-Me_2Pz)_2\}_2\{NP\Cl_2\}]$ (0.10 g, 0.22 mmol) in dichloromethane was added anhydrous PdCl₂(PhCN)₂ (0.08 g, 0.22 mmol), which was allowed to stir for 6 h at room temperature. It was then filtered and the filtrate concentrated to about 3 mL. To this was added 6 mL of *n*-hexane, which was kept at 0 °C to obtain a

Scheme 1



Scheme 2



crystalline product identified as **7**. Yield: 0.09 g (80%). Mp: 206 °C (d). UV/Visible: (CH₂Cl₂; λ_{max}/nm ($\epsilon_{max}/M^{-1}cm^{-1}$): 304 (2332), 281 (6024), 229 (22462). FT-IR ν/cm^{-1} : 3462 (b), 1679 (s), 1584 (s), 1409 (m), 1261 (m), 1093 (m), 804 (s), 532 (m). 1H NMR: 2.25, 2.39, 2.44 (s, 18H, Pz-CH₃), 5.68 (s, 3H, Pz-CH). ^{31}P NMR: 1.0 (s). Anal. Calcd for C₁₇H₂₁N₉POPdCl: C, 37.79; H, 3.92; N, 23.33. Found: C, 37.42; H, 3.62; N, 23.46.

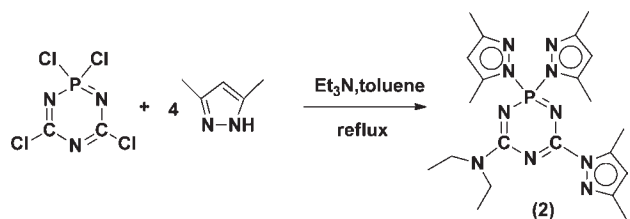
$[\{NC(3,5-Me_2Pz)NHC(3,5-Me_2Pz)\}_2\{NP(O)\}_2]$ (**9**). To a solution of $[\{NC(3,5-Me_2Pz)_2\}_2\{NP\Cl_2\}]$ (0.12 g, 0.25 mmol) in dichloromethane was added anhydrous K₂PtCl₄ (0.11 g, 0.26 mmol), which was allowed to stir for 6 h at room temperature. It was then filtered and the filtrate concentrated to about 3 mL. To this was added 6 mL of *n*-hexane, which was kept at 0 °C to obtain a crystalline product identified as **9**. Yield: 0.06 g (77%). Mp: 120 °C (d). FT-IR ν/cm^{-1} : 2929 (b), 1714 (s), 1606 (s), 1423 (m), 1074 (m), 972 (m), 716 (m), 494 (m). 1H NMR: 2.30, 2.39, 2.57 (s, 12H, Pz-CH₃), 5.71 (s, 2H, Pz-CH). ^{31}P NMR: -0.6 (s). Anal. Calcd for C₂₄H₃₀N₁₄P₂O₃: C, 46.16; H, 4.84; N, 31.40. Found: C, 46.20; H, 4.64; N, 31.55.

$[\{NC(OC_5H_4N)\}_2\{NP(NC(NMe_2)_2)_2\} \cdot \{PdCl_2\}]$ (**10**). To a solution of **4** (0.10 g, 0.19 mmol) in acetonitrile (40 mL) was added Pd(CH₃CN)₂Cl₂ (0.05 g, 0.19 mmol). After stirring for 12 h at room temperature in a N₂ atmosphere, the reaction mixture was filtered, concentrated to a volume of 10 mL, and kept for slow evaporation. After 7 days, yellow colored crystals were obtained. Yield: 0.83 g (62%). Mp. 250 °C. $^{31}P\{^1H\}$ NMR: δ 36.4 (s). ESI-MS m/z , ion: 692.10. IR (KBr) cm^{-1} : 3436 (b), 3112 (w), 2935 (w), 1641 (m), 1596 (s), 1521 (s), 1467 (m), 1405 (s), 1347 (s), 1321 (s), 1207 (m), 1131 (s), 1065 (w), 976 (s), 918 (m), 854 (m), 801 (m), 726 (m), 684 (m), 549 (m). Anal. Calcd. for C₂₂H₃₂Cl₂PdN₁₁PO₂ (689.09): C, 38.25; H, 4.67; N, 22.30. Found: C, 38.32; H, 4.74; N, 22.13.

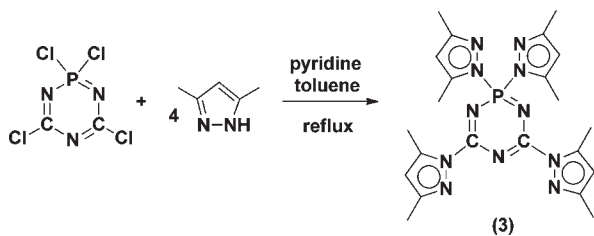
RESULTS AND DISCUSSION

Synthetic Aspects. The tetrachlorocarbophosphazene $[\{NC\Cl\}_2\{NP\Cl_2\}]$ was prepared according to a literature procedure.⁸ Reaction of $[\{NC\Cl\}_2\{NP\Cl_2\}]$ with $Me_2NCH_2NMe_2$ proceeds in a regioselective manner to afford $[\{NC(NMe_2)_2\}_2\{NP\Cl_2\}]$. In the latter, while the carbon centers are blocked, the phosphorus atom contains two reactive P–Cl bonds, which can be elaborated readily^{8,10} (Scheme 1). Accordingly, the reaction of $[\{NC(NMe_2)_2\}_2\{NP\Cl_2\}]$ with two equivalents of the sodium salt of 3,5-dimethylpyrazole in THF afforded the compound $[\{NC(NMe_2)_2\}_2\{NP(3,5-Me_2Pz)_2\}]$ (**1**; Scheme 2). On the other hand, the reaction of $[\{NC\Cl\}_2\{NP\Cl_2\}]$ with 4 mol of 3,5-dimethylpyrazole in the presence of triethylamine,

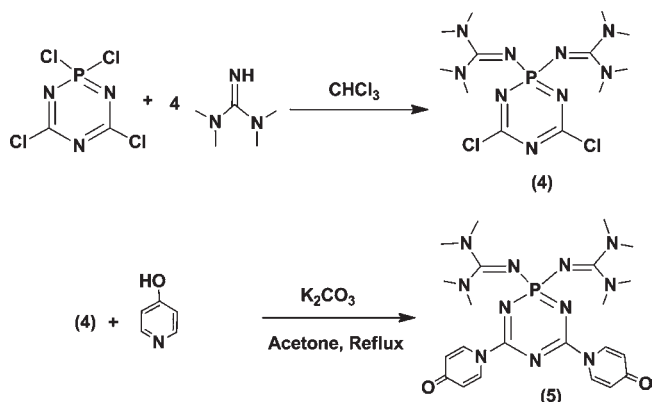
Scheme 3



Scheme 4



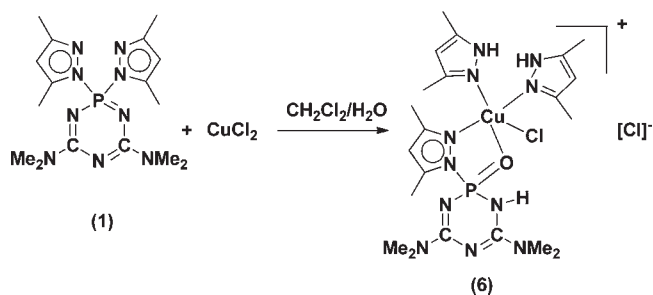
Scheme 5



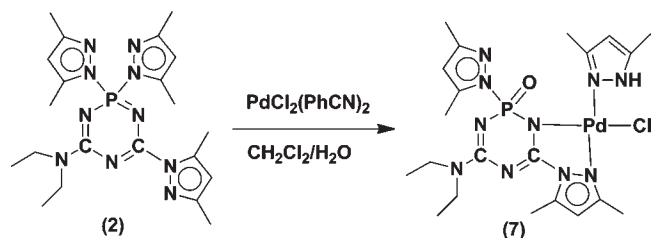
in refluxing toluene, afforded $[\{NC(NEt_2)\}_2\{NC(3,5-Me_2Pz)\}_2\{NP(3,5-Me_2Pz)_2\}_2]$ (2). Interestingly, in 2, one of the carbon centers contains a diethyl amino substituent formed as a result of a dealkylation reaction involving triethylamine (Scheme 3). The tetrakis pyrazolyl derivative, $[\{NC(3,5-Me_2Pz)\}_2\{NP(3,5-Me_2Pz)_2\}_2]$, was prepared by changing the HCl scavenger to pyridine (Scheme 4).

Since regioselective reactions could be readily brought out at the carbon center of $[\{NCCl\}_2\{NP(Cl)_2\}]$ in reactions with trialkylamines (by dealkylation reactions), we were in search of reagents that would result in regioselective substitution reactions at the phosphorus center leaving behind a product that would contain reactive C–Cl bonds. During this investigation, we found out that the reaction of $[\{NCCl\}_2\{NP(Cl)_2\}]$ with 1,1,3,3-tetramethyl-guanidine proceeds with regioselectivity at the phosphorus center, affording $[\{NCCl\}_2\{NP(NC(NMe_2)_2)_2\}]$ (4; Scheme 5). The C–Cl bonds in the latter could be replaced by appropriate reagents. Accordingly, the reaction of 4 with the potassium salt of 4-hydroxypyridine in acetone afforded the compound $[NC(p-OC_5H_4N)]_2[NP\{CN(NMe_2)_2\}_2]$ (5).

Scheme 6



Scheme 7



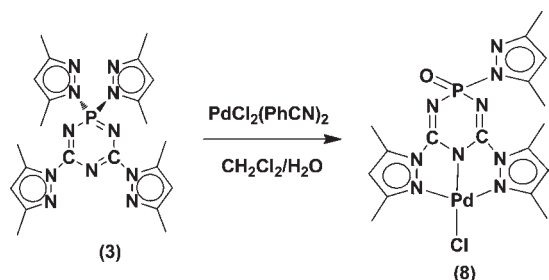
Interestingly, in 5, the deprotonated hydroxy pyridine ligand is connected to the carbon center at the nitrogen end of the ligand rather than at the oxygen end, underscoring the preference for the C–N bond formation in these reactions (Scheme 5).

Compounds 1–5 have been characterized by multinuclear NMR, Mass and X-ray crystallography. The ³¹P{¹H} NMR spectra of 1–5 are characterized by the presence of singlets at +24.0, +22.7, +22.4, −3.9, and +1.5 ppm, respectively. The chemical shifts of the pyrazolyl derivatives 1, 2, and 3 are upfield shifted in comparison to $[\{NCCl\}_2\{NP(Cl)_2\}]$ (+54.8 ppm),⁸ a trend that was also seen in cyclophosphazenes: N₃P₃Cl₆ (s, 19.3 ppm) and N₃P₃(3,5-Me₂Pz)₆ (s, −3.4 ppm).¹² Remarkably, the ³¹P NMR signals of the guanidine derivatives 4 and 5 are even further upfield shifted. FAB and ESI mass spectra of 1–5 indicate the presence of strong parent ion (M⁺) peaks: 376 (for 1), 455 (for 2), 478 (for 3), 396 (for 4), and 514 (for 5).

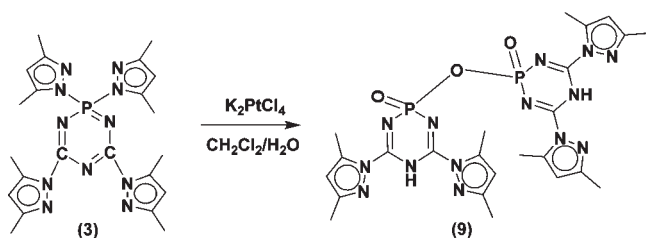
The reaction of 1 with CuCl₂ in dichloromethane containing adventitious moisture afforded the complex $[\{(O)P(3,5-Me_2Pz)_2\}N_3C_2(3,5-Me_2Pz)_2](3,5-Me_2Pz)_2CuCl]$ (6). The formation of 6 occurs via a P–N bond cleavage reaction. The resulting “free” pyrazole is found to coordinate to the metal center. This process results in the conversion of the cyclocarbophosphazene to cyclocarbophosphazane (Scheme 6). This type of hydrolytic cleavage of the P–N bonds was also observed during the metalation of $[\{NC(3,5-Me_2Pz)\}_2\{NP(3,5-Me_2Pz)_2\}]$,⁶ N₃P₃(3,5-Me₂Pz)₆,¹² (O)P(3,5-Me₂Pz)₃,¹³ MeP(S)(3,5-Me₂Pz)₂,¹⁴ PhP(O)(3,5-Me₂Pz)₂,¹⁵ and Ph₂P(O)(3,5-Me₂Pz).¹⁵ In each of these cases, it has been suggested that coordination of the ligand to the metal ion accentuates the electrophilicity at the phosphorus center, rendering it susceptible to nucleophilic attack.

In accordance with this expectation, the reaction of 2 with PdCl₂(PhCN)₂ afforded complex 7 (Scheme 7). Also, when $[\{NC(3,5-Me_2Pz)\}_2\{NP(3,5-Me_2Pz)_2\}]$ is allowed to react with PdCl₂(PhCN)₂, the P–N_{pz} bond is cleaved, affording 8 (Scheme 8). These reactions are reminiscent of the one involving $[\{NC(3,5-Me_2Pz)\}_2\{NP(3,5-Me_2Pz)_2\}]$ with CuCl₂ or CuBr₂,

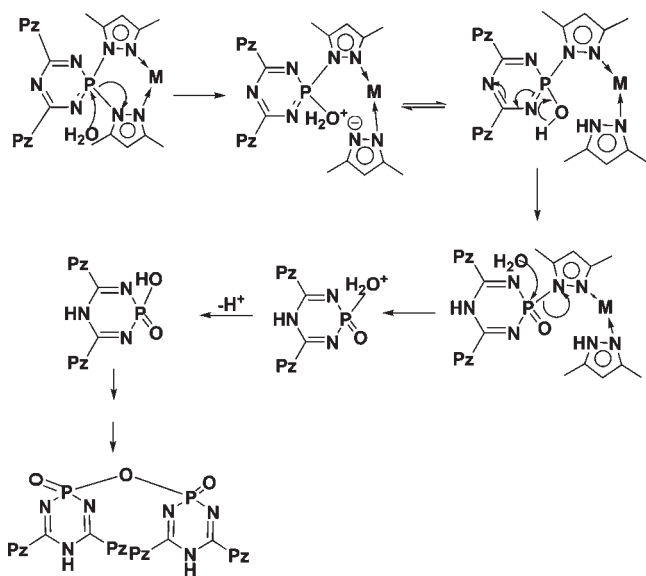
Scheme 8



Scheme 9



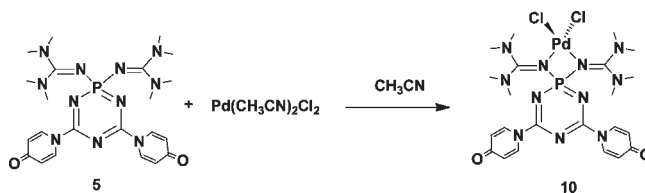
Scheme 10



which afforded tetranuclear ensembles, $[\{\{\text{NC}(3,5\text{-Me}_2\text{Pz})\}_2\{\text{NP}(\text{O})\}(\text{CuCl})\}_2\text{O}]_2$ and $[\{\{\text{NC}(3,5\text{-Me}_2\text{Pz})\}_2\{\text{NP}(\text{O})\}(\text{CuBr}_2)\}_2\text{O}]\{\{\text{NC}(3,5\text{-Me}_2\text{Pz})\}_2\{\text{NP}(\text{O})\}(\text{Cu}(3,5\text{-Me}_2\text{PzH}))\}_2]$; in these Cu(II) complexes, the P–N bonds are also hydrolyzed, while the C–N_{pz} bonds are intact and are involved in coordination to the copper ion.⁶

Reaction of $[\{\{\text{NC}(3,5\text{-Me}_2\text{Pz})\}_2\{\text{NP}(3,5\text{-Me}_2\text{Pz})_2\}]$ with K_2PtCl_4 leads to complete hydrolysis at the phosphorus center and results in a P–O–P bridged dimer, $[\{\{\text{NC}(3,5\text{-Me}_2\text{Pz})\}_2\{\text{NP}(\text{O})\}(\text{OH})\}_2]$ (9) (Scheme 9), which occurs as a result of the intermolecular condensation between two molecules of the in situ generated intermediate $[\{\{\text{NC}(3,5\text{-Me}_2\text{Pz})\}_2\{\text{NP}(\text{O})\}(\text{OH})\}]$ (Scheme 9).

Scheme 11



The mechanism of formation of 9 is proposed to proceed via an initial coordination of the metal ion with the $[\text{P}(3,5\text{-Me}_2\text{Pz})_2]$ motif. Nucleophilic attack by water at the phosphorus center results in the formation of a carbophosphazene containing a $[\text{P}(\text{O})(\text{OH})]$ unit, the eventual condensation of which leads to the formation of 9. P–O–P bridged products have been isolated, as mentioned above, in the reactions of $[\{\{\text{NC}(3,5\text{-Me}_2\text{Pz})\}_2\{\text{NP}(3,5\text{-Me}_2\text{Pz})_2\}]$ with $\text{CuCl}_2/\text{CuBr}_2$.⁶ It is also worth mentioning that the reaction of $\text{PhP}(\text{O})(3,5\text{-Me}_2\text{Pz})_2$ with Pd(II) salts results in the formation of $[\text{Pd}(3,5\text{-Me}_2\text{Pz})_3\text{Cl}]^+[\text{PhP}(\text{O})(\text{OH})\text{OP}(\text{O}_2)\text{Ph}]^-$.¹⁵ The anion of the latter also contains a P–O–P bond as in 9.

Instead of pyrazolyl carbophosphazene ligands when the 1,1,3,3-tetramethyl-guanidine substituted carbophosphazene $[\{\{\text{NC}(p\text{-OC}_5\text{H}_4\text{N})\}_2\{\text{NP}(\text{NC}(\text{NMe}_2)_2)_2\}]$ (5) was allowed to react with $\text{PdCl}_2(\text{CH}_3\text{CN})_2$ in acetonitrile, the desired complex, $[\{\{\text{NC}(\text{OC}_5\text{H}_4\text{N})\}_2\{\text{NP}(\text{NC}(\text{NMe}_2)_2)_2\} \cdot \{\text{PdCl}_2\}]$ (10; Scheme 11), was obtained, indicating the robustness of the P–N bond involved in this case. In this context, it must be mentioned that cyclophosphazene hydrazide ligands are also known to form hydrolytically stable metal complexes.¹⁶

The optical spectra of 6 and 7 show intense high-energy and weak low-energy absorptions. The low-energy bands occurring at 823 nm for 6 and 793 nm for 7 are attributed to d–d transitions. The bands at 331 (sh) nm for 6 and 386 nm (sh) for 7 are due to ligand–metal charge transfer. The high energy absorptions at 241 nm for 6 and 257 nm for 7 are due to intra-pyrazole $\pi\text{--}\pi^*$ transitions.

The EPR spectrum of the copper complex 6 has been recorded in solution both at room temperature and at 77 K. While the spectrum at room temperature is not particularly informative, the EPR spectrum recorded at 77 K shows an axial symmetry with $g_{\parallel} > g_{\perp}$. The g_{\parallel} value is 2.27, while the g_{\perp} value is 2.08. The A_{\parallel} value is $130 \times 10^{-4} \text{ cm}^{-1}$. These data are comparable to the Cu(II) complexes of pyrazolyl cyclophosphazenes where the Cu(II) center has a distorted trigonal bipyramidal geometry.¹⁷ For example, in $\text{N}_3\text{P}_3(3,5\text{-Me}_2\text{Pz})_6 \cdot \text{CuCl}_2$, the g_{\parallel} is 2.12, while g_{\perp} is 2.04. In $\text{N}_3\text{P}_3\text{Ph}_2(3,5\text{-Me}_2\text{Pz})_4 \cdot \text{CuCl}_2$, g_{\parallel} is 2.12 while g_{\perp} is 2.02.¹⁷

The ^{31}P NMR spectrum of 5 shows a singlet at 1.5 ppm. Surprisingly, this chemical shift in palladium complex 8 is relatively unaffected and is seen at 1.0 ppm. In contrast, because of the hydrolysis, the chemical shift of $[\{\{\text{NC}(3,5\text{-Me}_2\text{Pz})\}_2\{\text{NP}(3,5\text{-Me}_2\text{Pz})_2\}]$ which occurs at 22.4 ppm is upfield shifted to 36.4 in 7. The ^{31}P NMR spectrum of 9 shows a singlet at -0.6 ppm which is comparable to that found in 8, although in the latter the phosphorus atom contains a pyrazolyl and an oxo group. Palladium complex 10 shows a singlet in its $^{31}\text{P}\{^1\text{H}\}$ NMR at 36.4 ppm, which is considerably downfield shifted in comparison to the parent ligand 5 (1.5 ppm). The ESI-MS spectrum of this compound shows the parent ion at m/z 692.10, underscoring the stability of this complex in solution.

The molecular structures of 1–10 were confirmed by X-ray crystallography as discussed in the next section.

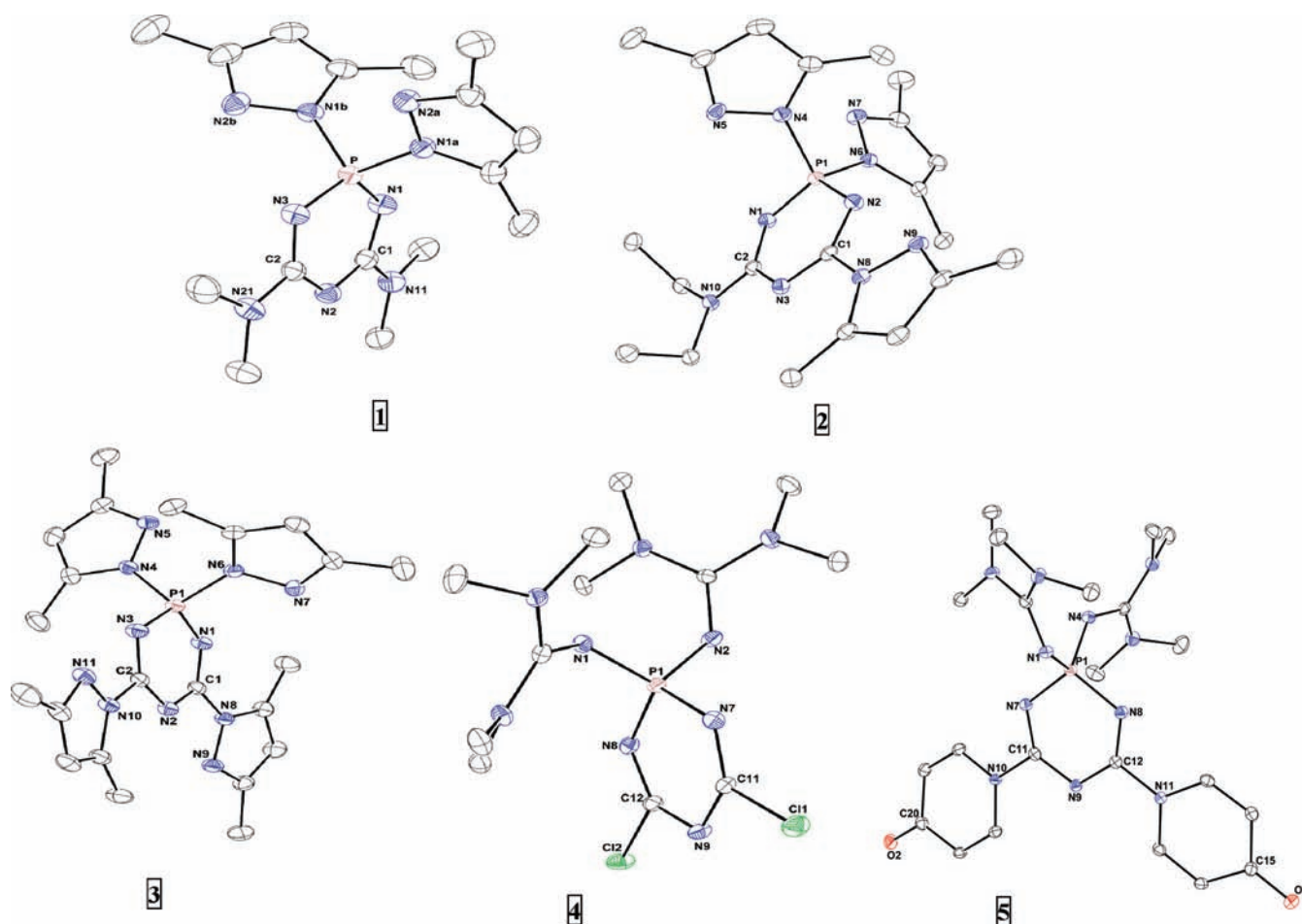


Figure 1. ORTEP diagrams of 1–5. Thermal ellipsoids are set at 30%, and hydrogen atoms have been omitted for clarity. Selected bond distances (Å) and bond angles (deg) for 1–5 are as follows. For 1: P–N3 = 1.578(2), C2–N3 = 1.346(3), C2–N2 = 1.348(3), P–N1 = 1.584(2), C1–N2 = 1.346(3), C1–N1 = 1.357(3), C1–N11 = 1.340(3), C2–N21 = 1.349(3), P–N1a = 1.7000(19), P–N1b = 1.690(2), N3–P–N1 = 115.32(11), P–N1–C1 = 114.87(16), N1–C1–N2 = 127.2(2), C1–N2–C2 = 119.157(2), N3–C2–N2 = 128.2(2), P–N3–C2 = 114.50(16). For 2: P1–N1 = 1.5806(13), C2–N1 = 1.3515(18), C2–N3 = 1.3722(18), C1–N3 = 1.3232(18), C1–N2 = 1.3319(18), P1–N2 = 1.6007(12), P1–N4 = 1.6810(13), P1–N6 = 1.6852(12), C2–N10 = 1.3429(18), C1–N8 = 1.4157(18), N1–P1–N2 = 114.27(7), C1–N2–P1 = 113.71(10), N2–C1–N3 = 130.73(13), C2–N3–C1 = 118.00(12), N1–C2–N3 = 126.73(12), P1–N1–C2 = 115.70(10), N4–P1–N6 = 101.37(6). For 3: P1–N1 = 1.5977(14), P1–N3 = 1.6011(14), C1–N1 = 1.327(2), C2–N3 = 1.330(2), C1–N2 = 1.340(2), C2–N2 = 1.334(2), N1–P1–N3 = 113.26(7), N1–C1–N2 = 129.52(15), N2–C2–N3 = 129.90(14), P1–N1–C1 = 114.87(11), P1–N3–C2 = 114.60(11), C1–N2–C2 = 117.31(13). For 4: P1–N8 = 1.6605(3), N8–C12 = 1.2882(5), N9–C12 = 1.3463(4), N9–C11 = 1.3453(4), N7–C11 = 1.2778(5), P1–N7 = 1.6616(3), P1–N1 = 1.5954(3), P1–N2 = 1.6001(3), C11–C11 = 1.7873(3), C12–C12 = 1.7777(3), N8–P1–N7 = 106.18(14), C11–N7–P1 = 117.3(2), N7–C11–N9 = 133.8(3), C11–N9–C12 = 111.9(3), N8–C12–N9 = 133.4(3), C12–N8–P1 = 117.3(2), N1–P1–N2 = 111.11(14). For 5: P1–N8 = 1.6594(19), N8–C12 = 1.301(3), N9–C12 = 1.344(3), N9–C11 = 1.350(3), N7–C11 = 1.294(3), P1–N7 = 1.6492(18), N10–C11 = 1.435(3), N11–C12 = 1.447(3), P1–N4 = 1.5987(19), P1–N1 = 1.6073(19), O1–C15 = 1.258(3), O2–C20 = 1.245(3), N7–P1–N8 = 106.17(9), C11–N7–P1 = 119.03(15), N7–C11–N9 = 130.78(19), C12–N9–C11 = 114.39(17), N8–C12–N9 = 131.70(19), C12–N8–P1 = 117.86(15), N4–P1–N1 = 107.67(9).

X-Ray Crystallography. *Molecular Structures of the Carbo-phosphazene Ligands 1–5.* The molecular structures of the carbophosphazene ligands 1–5 are given in Figure 1. The bond parameters of these compounds are summarized in the figure caption. In each of these compounds, the carbophosphazene ring is planar with very minor deviations from the mean plane of the ring by the constituent atoms (see the Supporting Information).

A comparison of the bond parameters of 1–5 is presented in Table 3. Expectedly, the bond parameters of the pyrazolyl derivatives 1–3 follow similar trends, while 4–5 show some variations in comparison to the former. The P–N_{ring} distances (average values) fall in the range 1.581(2)–1.600(3) Å. This value, which is shorter than the single bond P–N distance of

1.70 Å,¹⁸ is comparable to that found in pyrazolyl cyclophosphazenes. For example, the comparable ring P–N bond distance in *spiro*-N₃P₃[HN(CH₂)₃NH]](3,5-Me₂Pz)₄ is 1.578 (4) Å.¹⁹ The exocyclic P–N distances in 1–3 are longer than the endocyclic distances, and this trend is also similar to that found earlier in pyrazolyl cyclophosphazenes.^{4c,12,17} In contrast to the situation with P–N distances, the difference between the exo- and endocyclic C–N distances in 1–3 is not too different. The C–N distances observed in the present instance (Figure 1, Table 3) are shorter than the normal C–N single bond distance of 1.474 Å.²⁰ The angles at phosphorus in 1–3 are substantially smaller than those at carbon, a trend which is found in other cyclophosphazenes also.⁵ Similarly, in comparison to

Table 3. Comparison of Bond Lengths [Å] and Bond Angles [deg] of 1–5

	1	2	3	4	5
P–N _{exo}	1.695(2)	1.683(1)	1.674(2)	1.598(3)	1.603(2)
P–N _{ring}	1.581(2)	1.591(1)	1.600(3)	1.661(3)	1.654(2)
C–N _{ring} ^a	1.352(3)	1.342(2)	1.329(2)	1.283(5)	1.298(3)
C–N _{ring}	1.347(3)	1.323(2)	1.337(2)	1.346(4)	1.347(3)
		1.372(2)			
C–N _{exo}	1.340(3)	1.343(2)	1.399(1)		1.441(3)
	1.349(3)	1.416(2)			
N–P–N _{ring}	115.3(1)	114.3(1)	113.3(7)	106.2(1)	106.2(1)
N–C–N _{ring}	127.7(2)	128.7(1)	129.7(2)	133.6(1)	131.2(2)
P–N–C _{ring}	114.6(2)	114.7(1)	114.7(1)	117.3(1)	119.0(2)
C–N–C _{ring}	119.2(2)	118.0(1)	117.3(1)	111.9(1)	114.4(2)

^aThese C–N distances correspond to those that are adjacent to the P–N bond.

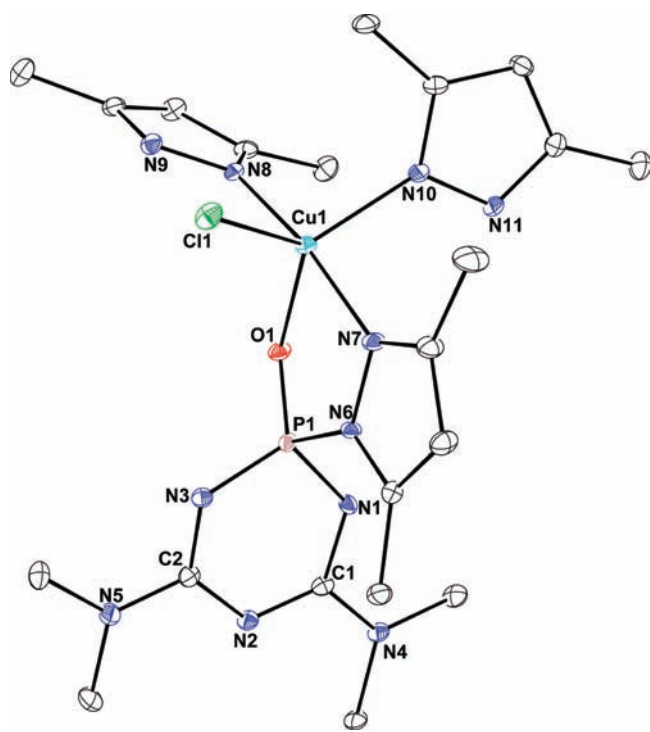


Figure 2. ORTEP diagram of **6**. Thermal ellipsoids are set at 30%, and hydrogen atoms have been omitted for clarity. Selected bond distances (Å) and bond angles (deg) are as follows: P1–N3 = 1.575(2), C2–N3 = 1.351(3), C2–N2 = 1.358(3), C1–N2 = 1.309(3), C1–N1 = 1.374(3), P1–N1 = 1.650(2), C1–N4 = 1.347(3), C2–N5 = 1.337(3), P1–O1 = 1.4813(16), P1–N6 = 1.7245(2), Cu1–Cl1 = 2.3307(7), Cu1–O1 = 2.0993(15), Cu1–N7 = 1.9931(19), Cu1–N10 = 2.036(2), Cu1–N8 = 1.9801(20), N3–P1–N1 = 106.227(11), P1–N1–C1 = 121.41(16), N1–C1–N2 = 124.0(2), C1–N2–C2 = 120.07(19), N3–C2–N2 = 126.94(2), P1–N3–C2 = 120.61(16), N7–Cu1–N8 = 169.78(8), O1–Cu1–N10 = 119.15(7), O1–Cu1–Cl1 = 119.78(5), Cl1–Cu1–N10 = 120.85(6).

P–N–C angles, C–N–C angles are slightly wider. In contrast to **1–3**, in the guanidine substituted compounds **4** and **5**, there is a reversal of trends in P–N bond distances. The exocyclic P–N bond distance is substantially shorter, suggesting extensive negative hyperconjugation involving the exocyclic nitrogen lone

pair and the P–N σ^* orbitals.²¹ Also, the C–N ring distances involving the nitrogen adjacent to phosphorus is shorter in comparison to the other bond.

Compound **5** is formed in the reaction of 4-hydroxypyridine with **4**. The reaction occurs at the nitrogen site rather than at oxygen. This is verified by the observed bond parameters in **5** where the C–N_{exo} distance is quite close to the expected C–N single bond distance. Further, the C–O distance [1.249(5); Table 3] is also consistent with a C=O bond distance.²²

Molecular Structures of 6–8 Containing Carbophosphazane Motifs. Compound **6**, a monocationic complex, [$\{\text{NC}(\text{NMe}_2)\}_2\{\text{NHP}(\text{O})(3,5\text{-Me}_2\text{Pz})\} \cdot \{\text{Cu}(3,5\text{-Me}_2\text{PzH})_2(\text{Cl})\}^- [\text{Cl}]$] (Figure 2) is formed as a result of P–N bond hydrolysis that accompanies metallation; the pyrazole ligands released after hydrolysis are transferred to the copper center. As a result of this hydrolysis, the inorganic ring is formally now a cyclocarbophosphazane ring, with the ring N1 nitrogen being protonated. Examples of such formal saturation in the ring structure are known among cyclophosphazenes²³ but are quite rare in the cyclocarbophosphazene family.

The ligand binds to copper in **6** in a bidentate manner through an intact pyrazole group and an oxygen atom (both of these substituents being present on the phosphorus center of the carbophosphazene), affording a five-membered CuN₂OP ring; the phosphorus atom serves as the common atom at the spirocyclic junction between the six-membered and the five-membered rings (Figure 2). The coordination environment around copper is 3N, 1O, 1Cl, and the geometry around it is slightly distorted trigonal bipyramidal (Figure 2). The pyrazolyl pyridinic nitrogen (N7) from carbophosphazene and the pyrazolyl pyridinic nitrogen (N8) from the free pyrazole take up the axial positions. The axial N(7)–Cu(1)–N(8) angle is 169.78(7)°, while the equatorial angles N(10)–Cu(1)–O(1), N(10)–Cu(1)–Cl(1), and Cl(1)–Cu(1)–O(1) are 119.15(7), 120.85(6), and 119.78(5)°, respectively. The Cu–N bond distances are nearly similar [Cu(1)–N(7), 1.993(2); Cu(1)–N(8), 1.980(2); Cu(1)–N(10), 2.036(2) Å], while the Cu–O [2.099(2) Å] and Cu–Cl [2.331(1) Å] distances are in keeping with literature precedents.¹⁴ Complex **6** is the first example, to the best of our knowledge, where a formal P=O unit of a cyclophosphazene or a carbophosphazene ligand is involved in bonding to Cu(II). The bond distances of the inorganic heterocyclic ring undergo changes as a result of metalation. Thus, the two ring P–N distances are now nonequivalent [P–N1 = 1.650(2) and P–N3 = 1.575(2) Å] as a result of protonation at N1. Expectedly, the C–N distances are not affected by metalation.

The crystal structure of **6** shows the presence of interesting chloride–dichloromethane dimers $\{\text{Cl}^- \cdots \text{HClCClH} \cdots \text{Cl}^-\}$ as a result of hydrogen bonding interactions between the chloride anions and the solvent dichloromethane (Figure 3). These clusters contain C–H \cdots Cl interactions and are reminiscent of the recently reported chloride–chloroform clusters.²⁴ Such clusters have important mechanistic implications, particularly in nucleophilic substitution reactions; the hydrogen bonded structures have been suggested as possible models for intermediates containing an incipient nucleophile and a leaving group. The weak interactions found in **6** lead to the formation of a supramolecular tape. The hydrogen-bond parameters found in **6** are summarized in Table 4.

In compound **7**, the ligand again undergoes a P–N bond scission after metalation to generate a cyclocarbophosphazane

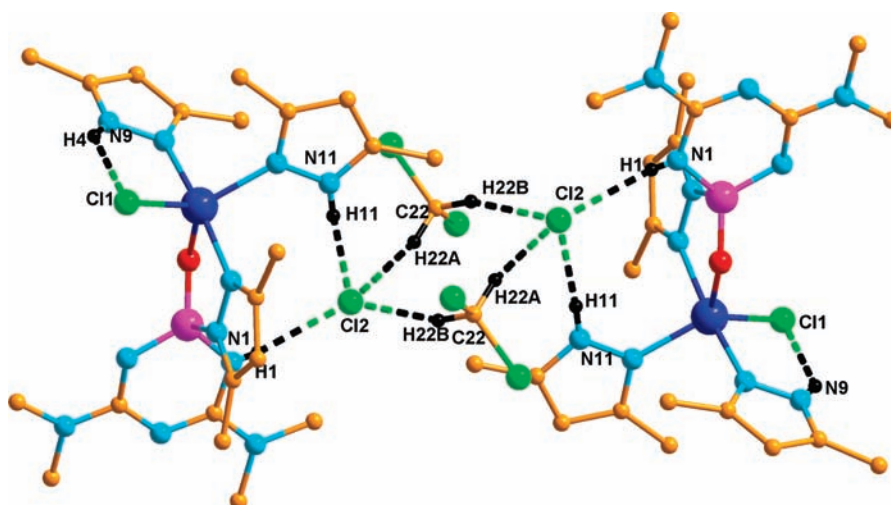


Figure 3. Hydrogen bonding interactions between the chloride anion and dichloromethane solvent in **6**, leading to the formation of a supramolecular tape.

Table 4. Hydrogen-Bond Parameters Found in $[\{\text{NC}(\text{NMe}_2)\}_2\{\text{NHP}(\text{O})(3,5\text{-Me}_2\text{Pz})\} \cdot \{\text{Cu}(3,5\text{-Me}_2\text{PzH})_2\text{-}(\text{Cl})\}][\text{Cl}]$ (**6**)^a

D—H···A	<i>d</i> (H···A), Å	<i>d</i> (D···A), Å	∠(DHA), deg
N(1)—H(1)···Cl(2)	2.515(21)	3.129(22)	163.543(26)
N(11)—H(11)···Cl(2)	2.287(25)	3.149(20)	176.008(23)
N(9)—H(4)···Cl(1)	2.517(25)	3.059(24)	133.801(23)
C(22)—H(22A)···Cl(2)	2.678(7)	3.608(26)	156.530(14)
C(22)—H(22B)···Cl(2)	2.572(6)	3.525(22)	161.613(14)

^aSymmetry transformations used to generate equivalent atoms: $-x, 1 - y, 1 - z$.

moiety, $[\{\text{NC}(\text{NEt}_2)_2\}\{\text{NC}(3,5\text{-Me}_2\text{Pz})\}\{\text{NP}(\text{O})(3,5\text{-Me}_2\text{Pz})\}]$, which binds to Pd(II) in a bidentate manner (Figure 4). The essential difference between **6** and **7** is that the inorganic ring binds to Pd(II) through a pyrazole arm connected to a carbon atom and a ring nitrogen atom; the pyrazole moiety attached to phosphorus remains uncoordinated. The varied coordination behavior of the ligand in **6** and **7** is indicative of its ability to adjust to the coordination needs of the transition metal ion involved. Coordination of the ring nitrogen atom and the pyrazole unit to Pd(II) in **7** generates a five-membered PdN₃C ring which has a common edge with the carbophosphazene ring (Figure 4). The other two coordination sites around Pd(II) are taken up by a free pyrazole and a chloride ligand. The ring nitrogen atom bound to palladium arises from deprotonation of a NH group, affording charge neutrality. This assignment is confirmed by the P—N bond nonequivalence [P1—N1, 1.671 (1); P1—N2, 1.600 (7) Å]. Among the C—N distances, two are short [C1—N3, 1.317(10); C2—N2, 1.330 (11) Å] while two are longer [C1—N1, 1.363(10); C2—N3, 1.375(11) Å]. The P—O distances found in **6** and **7** [1.481(2) and 1.472(6) Å, respectively] are comparable to that found in $[\text{NC}(\text{N}(\text{Et})_2)_2][\text{NHP}(\text{O})(\text{Cl})]$, 1.471(2) Å.²⁵

The molecular structure of **8** is shown in Figure 5. In this compound also the cyclocarbophosphazene ligand is converted into a cyclocarbophosphazane after metalation. However, in **8**, the ligand binds in a η^3 -nongeminal mode: two of the pyrazole arms present on the two carbon centers of the ligand along with

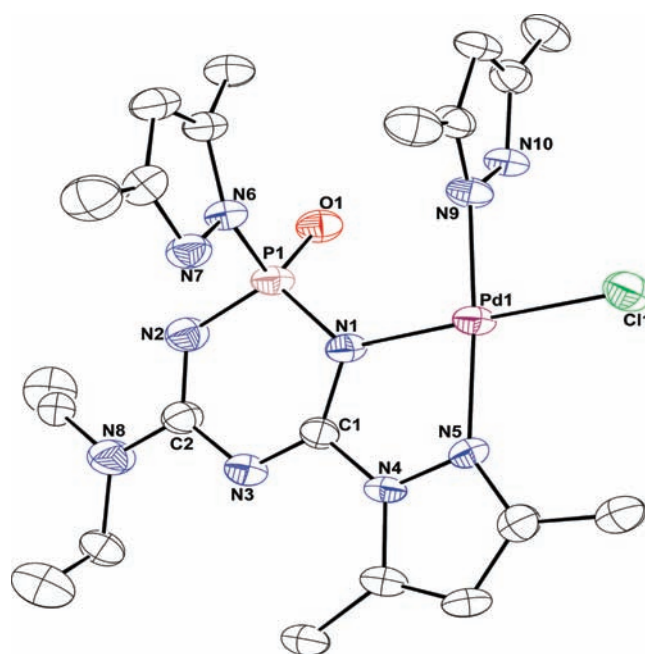


Figure 4. ORTEP diagram of **7**. Thermal ellipsoids are set at 30%, and hydrogen atoms have been omitted for clarity. Selected bond distances (Å) and bond angles (deg) are as follows: P1—N2 = 1.600(7), C2—N2 = 1.330(11), C2—N3 = 1.375(11), C1—N3 = 1.317(10), C1—N1 = 1.363(10), P1—N1 = 1.671(7), C2—N8 = 1.3407(12), C1—N4 = 1.4030(9), P1—N6 = 1.7022(7), P1—O = 1.472(6), Pd—N1 = 2.026(6), Pd—N9 = 1.992(7), Pd—N5 = 2.000(6), Pd—Cl = 2.296(2), N1—P1—N2 = 107.5(4), P1—N1—C1 = 116.1(5), N1—C1—N3 = 130.9(7), C1—N3—C2 = 116.95(7), N3—C2—N2 = 126.7(2), C2—N2—P1 = 121.75(6), O—P1—N6 = 107.015(33), N9—Pd—N5 = 175.9(3), N1—Pd—Cl = 178.5(2), N1—Pd—N5 = 80.27(23), N1—Pd—N9 = 95.6(3).

the ring nitrogen atom present in between them act in a concerted binding mode to hold palladium. The fourth coordination position on palladium is taken up by a chloride ligand. The ring nitrogen atom that binds to palladium is, like in **7**, anionic. The formation of the palladium complex leads to the simultaneous generation of two five-membered PdN₃C rings (Figure 5).

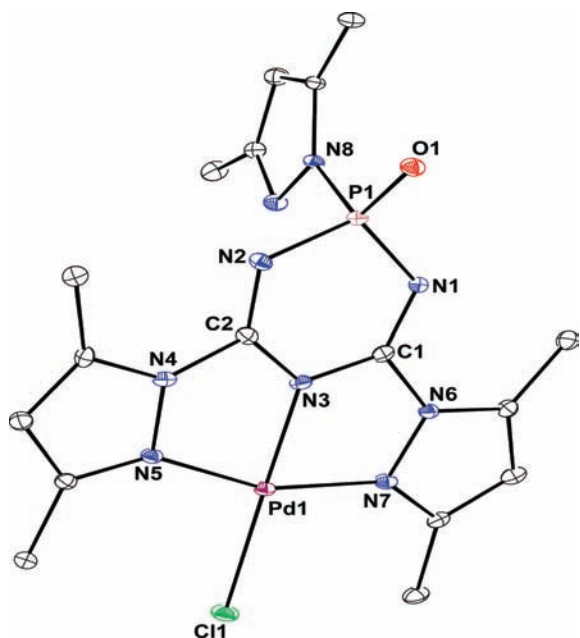


Figure 5. ORTEP diagram of **8**. Thermal ellipsoids are set at 30%, and hydrogen atoms have been omitted for clarity. Selected bond distances (Å) and bond angles (deg) are as follows: P1–N2 = 1.659(4), C2–N2 = 1.285(4), C2–N3 = 1.35(5), C1–N3 = 1.356(5), C1–N1 = 1.277(5), P1–N1 = 1.655(3), P1–O1 = 1.465(3), P1–N8 = 1.7024(4), Pd1–N3 = 1.933(3), Pd1–N7 = 2.020(3), Pd1–N5 = 2.026(3), Pd1–C11 = 2.2949(12), N1–P1–N2 = 108.77(19), P1–N1–C1 = 117.2(3), N1–C1–N3 = 129.12(4), C1–N3–C2 = 118.59(3), N3–C2–N2 = 128.59(4), P1–N2–C2 = 117.34(3), N3–Pd1–C11 = 178.81(11), N5–Pd1–N7 = 159.37(13), N3–Pd1–N5 = 79.37(13), N3–Pd1–N7 = 80.00(15), O1–P1–N8 = 109.623(19).

As in the previous cases, **6** and **7**, in **8** also, the P–N bond is cleaved upon metalation, indicating that the first site of interaction is at the phosphorus-bound pyrazole center. Interestingly, the η^3 -*nongeminal* mode of binding observed in **8** is reminiscent of the coordination behavior exhibited by pyrazolyl cyclophosphazenes in its metal complexes such as $\text{N}_3\text{P}_3(3,5\text{-Me}_2\text{Pz})_6 \cdot \text{CuCl}_2$.¹⁷ Also, this mode of binding has been observed in the tetranuclear copper complexes $[\{\{\text{NC}(3,5\text{-Me}_2\text{Pz})\}_2\{\text{NP}(\text{O})\}(\text{CuCl})\}_2\text{O}]_2$ and $[\{\{\text{NC}(3,5\text{-Me}_2\text{Pz})\}_2\{\text{NP}(\text{O})\}(\text{CuBr}_2)\}_2\text{O}\{\{\text{NC}(3,5\text{-Me}_2\text{Pz})\}_2\{\text{NP}(\text{O})\}\{\text{Cu}(3,5\text{-Me}_2\text{PzH})\}\}_2]_2$.⁶

The geometry around palladium in **8** is distorted square planar with the two *trans* sites being occupied by the pyrazole nitrogen atoms and the other two by the ring nitrogen and the chloride ligand, respectively (Figure 5). The interaction of the ring nitrogen atom with palladium affects the C–N bond distances flanking this site: distances involving C2–N3 [1.35(5)] and C1–N3 [1.356(5)] are comparatively longer than those present in C1–N1 [1.277(5)] and C2–N2 [1.285(4)] Å. Similarly, the two P–N_{ring} distances are quite long: P1–N1 = 1.655(3) and P1–N2 = 1.659(4) Å, reflecting the cyclocarbophosphazane nature of the ring. The P–O bond distance of 1.465(3) Å is comparable to that found in **6** and **7**.

Molecular Structure of the P–O–P Containing Compound $[\{\{\text{NC}(3,5\text{-Me}_2\text{Pz})\}\{\text{NHC}(3,5\text{-Me}_2\text{Pz})\}\{\text{NP}(\text{O})\}\}_2]_2$ (**9**). Attempts to metalate **3** with K_2PtCl_4 afforded **9**, where two carbophosphazane units are linked to each other by a P–O–P linkage. In this case, we could not isolate any metal complex. The mechanism of formation of **9** has been discussed *vide supra*.

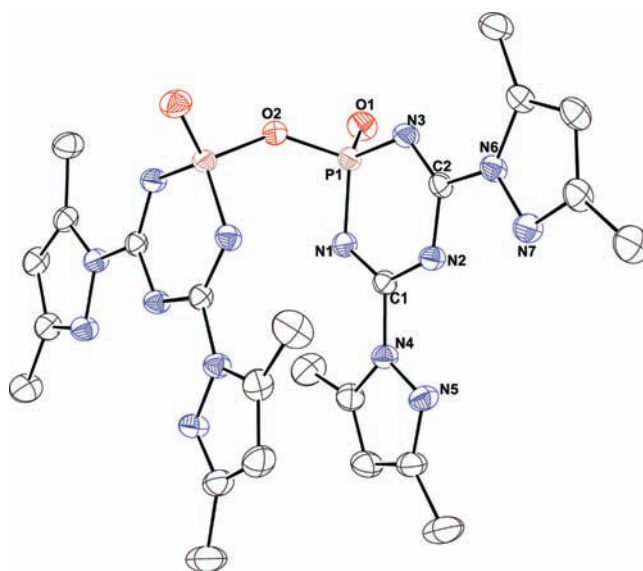


Figure 6. ORTEP diagram of **9**. Thermal ellipsoids are set at 30%, and hydrogen atoms have been omitted for clarity. Selected bond distances (Å) and bond angles (deg) are as follows: P1–N3 = 1.645(3), N3–C2 = 1.277(3), C2–N2 = 1.369(3), N2–C1 = 1.363(4), C1–N1 = 1.280(3), N1–P1 = 1.646(2), P1–O1 = 1.453(2), P1–O2 = 1.591(1), C1–N4 = 1.393(3), C2–N6 = 1.391(4), N3–P1–N1 = 108.68(11), P1–N1–C1 = 118.79(17), N1–C1–N2 = 125.997(22), C2–N2–C1 = 121.553(20), N2–C2–N3 = 125.45(21), C2–N3–P1 = 119.368(18), P1–O2–P1 = 141.777(38).

The molecular structure of **9** reveals two centrosymmetrically related subunits, each of which contains a cyclocarbophosphazane motif (Figure 6). Two types of P–O bonds are present corresponding to the structure of **9**: a shorter P–O distance, P1–O1, at 1.453(2) and a longer distance, P1–O2, at 1.591(1) Å. Within the carbophosphazane ring, the two P–N distances are comparable and long [P1–N1, 1.646(1) and 1.645(2) Å]. Among the C–N distances, two are short [C1–N1, 1.280(1); C2–N3, 1.277(3) Å] while two are long [C1–N2, 1.363(1); C2–N2, 1.369(1) Å] consistent with the structure of **9**.

Molecular Structure of $[\{\{\text{NC}(\text{OC}_5\text{H}_4\text{N})\}_2\{\text{NP}(\text{NC}(\text{NMe}_2)_2)_2\}\} \cdot \{\text{PdCl}_2\}]$ (**10**). The molecular structure of **10** is shown in Figure 7. In this compound, the carbophosphazane ligand functions as a 2N donor binding to Pd(II) through the two geminal guanidine nitrogen atoms to afford a four-membered PdN₂P ring. The most important aspect of this reaction is the *absence* of P–N bond hydrolysis during metalation. We have shown previously that cyclophosphazene hydrazides are resistant to hydrolysis even upon interaction with hydrated metal salts.¹⁶ It appears that guanidine-substituted cyclocarbophosphazenes are similarly robust. The third and fourth coordination sites around Pd(II) are taken up by two chloride ligands. The overall geometry around palladium is distorted square planar (Figure 7). An interesting effect of metalation on the bond parameters of **10** is a lengthening of the exocyclic P–N bond distances and a shortening of the endocyclic distances in comparison to that found in **5**. This is due to the fact that the lone pairs at the guanidine nitrogen are engaged in coordination to the metal ion rather than in negative hyperconjugation. This effect also influences the remote C–N bond distances: the C–N distances proximal

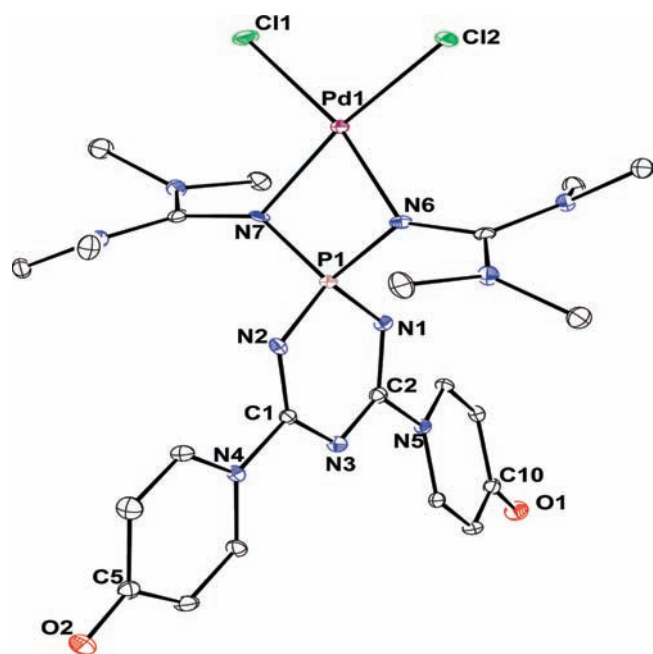


Figure 7. ORTEP diagram of **10**. Thermal ellipsoids are set at 30%, and hydrogen atoms have been omitted for clarity. Selected bond distances (Å) and bond angles (deg) are as follows: P1–N1 = 1.628(3), N1–C2 = 1.315(5), N3–C2 = 1.325(5), N3–C1 = 1.324(5), N2–C1 = 1.312(5), P1–N2 = 1.631(3), N4–C1 = 1.439(5), N5–C2 = 1.446(5), O1–C10 = 1.249(5), O2–C5 = 1.255(5), P1–N7 = 1.628(4), P1–N6 = 1.641(3), Pd1–N6 = 2.041(3), Pd1–N7 = 2.046(3), Pd1–Cl2 = 2.2922(11), Pd1–Cl1 = 2.2984(11), N1–P1–N2 = 108.11(18), C1–N2–P1 = 117.6(3), N2–C1–N3 = 130.2(4), C1–N3–C2 = 116.1(3), N1–C2–N3 = 130.7(4), C2–N1–P1 = 117.2(3), N7–P1–N6 = 92.94(17), N6–Pd1–N7 = 70.92(14), N6–Pd1–Cl1 = 167.94(10), N7–Pd1–Cl1 = 97.44(10), Cl2–Pd1–Cl1 = 93.07(4), N6–Pd1–Cl2 = 98.41(10), N7–Pd1–Cl2 = 169.10(10).

to the phosphorus center are slightly lengthened, while those that are distal are slightly shortened (Figure 7).

CONCLUSION

We have shown that cyclocarbophosphazene rings can be elaborated into various multisite coordination ligands by utilizing nucleophilic substitution reactions involving the C–Cl and/or the P–Cl bond. By a proper choice of the reagent, it is possible to direct the nucleophilic substitution reaction to occur either at the carbon or the phosphorus center, thereby increasing diversity among the resultant ligands. All of the pyrazolyl carbophosphazene ligands investigated in this study have been shown to undergo a regioselective P–N bond hydrolysis upon metalation, a feature which can be used as a synthetic tool. It is also possible to prepare hydrolytically stable cyclocarbophosphazene-supported ligands. Thus, guanidine-containing carbophosphazenes do not undergo hydrolysis upon metalation; the two guanidine arms on phosphorus are quite robust and are involved in a chelating coordination action with Pd(II). It appears that carbophosphazenes with two distinct centers of structure and reactivity, in the form of two planar carbon atoms and a tetrahedral phosphorus atom, provide intriguing possibilities for novel ligand design. These possibilities are further enriched by the subtle differences in P–N bond reactivity depending on the nature of the substituent. As a result, carbophosphazenes can be used as

scaffolds for supporting diverse ligand platforms which can exhibit rich coordination chemistry.

ASSOCIATED CONTENT

Supporting Information. Tables of bond parameters and mean planes. This material is available free of charge via the Internet at <http://pubs.acs.org>.

AUTHOR INFORMATION

Corresponding Author

*E-mail: vc@iitk.ac.in.

DEDICATION

*Dedicated to Prof. N. Sathyamurthy on the occasion of his 60th birthday.

ACKNOWLEDGMENT

We thank the Department of Science and Technology, India and the Council of Scientific and Industrial Research, India for financial support. VC is thankful for the Department of Science and Technology for a J. C. Bose fellowship. AD and RS thank IIT Kanpur and Council of Scientific and Industrial Research, India, for Senior Research Fellowships.

REFERENCES

- (1) (a) Chandrasekhar, V.; Krishnan, V. *Adv. Inorg. Chem.* **2002**, *53*, 159. (b) Allen, C. W. *Coord. Chem. Rev.* **1994**, *130*, 137. (c) Chivers, T.; Manners, I. *Inorganic Rings and Polymers of the p-Block Elements*; RSC Publishing: Cambridge, U. K., 2009. (d) Chandrasekhar, V. *Inorganic and Organometallic Polymers*; Springer-Verlag: Heidelberg, Germany, 2005. (e) Mark, J. E.; Allcock, H. R.; West, R. *Inorganic Polymers*, 2nd ed.; Oxford University Press: Toronto, Canada, 2005. (f) Gleria, M.; De Jaeger, R. *Applicative Aspects of Cyclophosphazenes*; Nova Science Publishers: New York, 2004.
- (2) Allen, C. W. *Chem. Rev.* **1991**, *91*, 119.
- (3) (a) McNally, L.; Allen, C. W. *Heteroatom Chem.* **1993**, *4*, 159. (b) Hayes, R. F.; Allen, C. W. *J. Inorg. Organomet. Polym. Mater.* **2010**, *20*, 528. (c) Carter, K. R.; Calichman, M.; Allen, C. W. *Inorg. Chem.* **2009**, *48*, 7476. (d) Chandrasekhar, V.; Athimoolam, A.; Srivatsan, S. G.; Sundaram, P. S.; Verma, S.; Steiner, A.; Zacchini, S.; Butcher, R. *Inorg. Chem.* **2002**, *41*, 5162. (e) Chandrasekhar, V.; Athimoolam, A. *Org. Lett.* **2002**, *4*, 2113. (f) Chandrasekhar, V.; Athimoolam, A.; Reddy, N. D.; Nagendran, S.; Steiner, A.; Zacchini, S.; Butcher, R. *Inorg. Chem.* **2003**, *42*, 51.
- (4) (a) Chandrasekhar, V.; Murugesapandian, B. *Acc. Chem. Res.* **2009**, *42*, 1047. (b) Chandrasekhar, V.; Thilagar, P.; Pandian, B. M. *Coord. Chem. Rev.* **2007**, *251*, 1045. (c) Steiner, A.; Zacchini, S.; Richards, P. I. *Coord. Chem. Rev.* **2002**, *227*, 193. (d) Chandrasekhar, V.; Nagendran, S. *Chem. Soc. Rev.* **2001**, *30*, 193. (e) Allcock, H. R.; Desorice, J. L.; Riding, G. H. *Polyhedron* **1987**, *6*, 119. (f) Horvath, R.; Otter, C. A.; Gordon, K. C.; Brodie, A. M.; Ainscough, E. W. *Inorg. Chem.* **2010**, *49*, 4073. (g) Boomishankar, R.; Richards, P.; Gupta, A. K.; Steiner, A. *Organometallics* **2010**, *29*, 2525. (h) Jimenez, J.; Laguna, A.; Benouazzane, M.; Sanz, J. A.; Diaz, C.; Valenzuela, M. L.; Jones, P. G. *Chem.—Eur. J.* **2009**, *15*, 13509. (i) Ainscough, E. W.; Brodie, A. M.; Davidson, R. J.; Moubaraki, B.; Murray, K. S.; Otter, C. A.; Waterland, M. R. *Inorg. Chem.* **2008**, *47*, 9182. (j) Bloy, M.; Kretschmann, M.; Scholz, S.; Teichert, M.; Diefenbach, U. *Z. Anorg. Allg. Chem.* **2000**, *626*, 1946.
- (5) (a) Behera, N.; Mishra, P. K.; Elias, A. J. *Phosphorus, Sulfur Silicon Relat. Elem.* **2006**, *181*, 2445. (b) Rivad, E.; Lough, A. J.; Chivers, T.; Manners, I. *Inorg. Chem.* **2004**, *43*, 802. (c) Reddy, N. D.; Elias, A. J.; Vij,

- A. *Inorg. Chem. Commun.* **2000**, 3, 29. (d) Elias, A. J.; Jain, M.; Reddy, D. N. *Phosphorus Sulfur Silicon Relat. Elem.* **1998**, 140, 203. (e) Vij, A.; Elias, J. A.; Kirchmeier, L. R.; Shreeve, M. J. *Inorg. Chem.* **1997**, 36, 2730. (f) Allcock, H. R.; Coley, S. M.; Manners, I.; Visscher, K. B.; Parvez, M.; Nuyken, O.; Renner, G. *Inorg. Chem.* **1993**, 32, 5088.
- (6) Chandrasekhar, V.; Azhakar, R.; Krishnan, V.; Athimoolam, M.; Pandian, B. M. *J. Am. Chem. Soc.* **2006**, 128, 6808.
- (7) *Vogel's Textbook of Practical Organic Chemistry*, 5th ed.; Longman: London, 1989.
- (8) Becke-Goehring, M.; Jung, D. *Z. Anorg. Allg. Chem.* **1970**, 372, 233.
- (9) Baumgarten, H. E. *Org. Synth. Coll.*; John Wiley: New York, 1973, 434.
- (10) Dastagiri Reddy, N.; Elias, A. J.; Vij, A. *J. Organomet. Chem.* **1999**, 580, 41.
- (11) (a) *SMART Software Reference manual*; *SAINT Software Reference manual*, version 6.45; Bruker Analytical X-ray Systems, Inc.: Madison, WI, 2003. (b) Sheldrick, G. M. *SADABS*, version 2.05; University of Göttingen: Göttingen, Germany, 2002. (c) *SHELXTL Reference Manual*, version 6.1; Bruker Analytical X-ray Systems, Inc.: Madison, WI, 2000. (d) Sheldrick, G. M. *SHELXTL*, version 6.12; Bruker AXS Inc.: Madison, WI, 2001. (e) Sheldrick, G. M. *SHELXL97*; University of Göttingen: Göttingen, Germany, 1997. (f) Bradenburg, K. *Diamond*, version 3.1eM; Crystal Impact GbR: Bonn, Germany, 2005.
- (12) Justin Thomas, K. R.; Chandrasekhar, V.; Scott, S. R.; Hallford, R.; Cordes, A. W. *J. Chem. Soc., Dalton Trans.* **1993**, 2589.
- (13) (a) Chandrasekhar, V.; Nagendran, S.; Kingsley, S.; Krishnan, V.; Boomishankar, R. *Proc. Ind. Acad. Sci. (Chem. Sci)* **2000**, 112, 171. (b) Joshi, V. S.; Kale, V. K.; Sathe, K. M.; Sarkar, A. *Organometallics* **1991**, 10, 2898.
- (14) Chandrasekhar, V.; Kingsley, S.; Vij, A.; Lam, K. C.; Rheingold, A. L. *Inorg. Chem.* **2000**, 39, 3238.
- (15) Kingsley, S.; Vij, A.; Chandrasekhar, V. *Inorg. Chem.* **2001**, 40, 6057.
- (16) Chandrasekhar, V.; Krishnan, V.; Steiner, A.; Bickley, J. F. *Inorg. Chem.* **2004**, 43, 166.
- (17) Justin Thomas, K. R.; Chandrasekhar, V.; Pal, P.; Scott, S. R.; Hallford, R.; Cordes, A. W. *Inorg. Chem.* **1993**, 32, 606.
- (18) Rademacher, P. In *Strukturen Organischer Moleküle*; VCH: Weinheim, Germany, 1987.
- (19) Cordes, W. A.; Folkert, S.; Bryan, D. C.; Chandrasekhar, V.; Thomas, R. J. *Acta Crystallogr.* **1994**, C50, 1976.
- (20) Katritzky, R. A.; Ghiviriga, I.; Steel, J. P.; Oniciu, C. D. *J. Chem. Soc., Perkin Trans. 2* **1996**, 443.
- (21) Murugavel, R.; Krishnamurthy, S. S.; Chandrasekhar, J.; Nethaji, M. *Inorg. Chem.* **1993**, 32, 5447.
- (22) Hocking, K. R.; Hambley, W. T. *Chem. Commun.* **2003**, 1516.
- (23) Richards, I. P.; Steiner, A. *Inorg. Chem.* **2005**, 44, 275.
- (24) (a) Denifl, S.; Zappa, F.; Mähr, I.; Mauracher, A.; Probst, M.; Märk, D. T.; Scheier, P. *J. Am. Chem. Soc.* **2008**, 130, 5065. (b) Gushchin, V. P.; Starova, L. G.; Haukka, M.; Kuznetsov, L. M.; Eremenko, L. I.; Kukushkin, Y. V. *Cryst. Growth Des.* **2010**, 10, 4839.
- (25) Dastagiri, N. R. Ph. D Thesis, 1999, Indian Institute of Technology, Kanpur, India.